THE ROLE OF PLASTICITY IN FATIGUE AND FRACTURE MECHANICS OF METALLIC MATERIALS

M. Chiarelli and A. Frediani
Dipartimento di Ingegneria Aerospaziale
Università di Pisa

M. Lucchesi
Dipartimento di Scienze e Storia dell'Architettura
Università di Chieti

Abstract

The definition of Crack Extension Energy Rate **G** for elasto-plastic materials with hardening is given here as a generalization of the Energy Release Rate; it is obtained by substituting the strain energy density with the work done by the internal forces. A procedure for the computation of **G**, starting from a finite element analysis of a cracked body, is then described in bidimensional problems. The results show that, in the case of cyclic loads, a certain decrease of **G** is produced and a crack closure is present with positive tensile loads, independently of the kinematics of the cracked faces; the results obtained depend on the constitutive characteristics of the materials.

I. Introduction

For a hyperelastic body, which is homogeneous and subject to quasi-static small deformations, and in the absence of body forces, the energy absorbed at the crack tip for unit crack extension, called Energy Release Rate, is [1],[2]

$$\mathbf{G}(l) = -\frac{d}{dl}\int_B \sigma\, da + \int_{\partial B} T\, \nu\cdot\mathbf{u}'\, ds \qquad (1)$$

where l, σ, T, ν, and $\mathbf{u}$ are the crack length, the strain-energy density, the Cauchy stress, the outward unit normal to ∂B and the displacement field, respectively. Moreover, in a bidimensional problem, if γ is a path around the tip, that is, a smooth non-intersecting path that starts and ends on the crack and surrounds the tip (Fig. 1), the quantity

$$J(\gamma) = \mathbf{e}\cdot\int_\gamma (\sigma I - \nabla\mathbf{u}^T T)\mathbf{n}\, ds \qquad (2)$$

where $\mathbf{e}$, I and $\mathbf{n}$ are the direction of propagation of the crack, the identity tensor and the outward unit normal on γ, respectively, is the J-integral corresponding to γ. The tensor $(\sigma I - \nabla\mathbf{u}^T T)$ is called the Energy Momentum Tensor[3]. As is well known, in this case we have

$$\mathrm{div}(\sigma I - \nabla\mathbf{u}^T T) = 0 \qquad (3)$$

and, thus, if the crack is straight,

$$\mathbf{G} = J(\gamma). \qquad (4)$$

A definition of **G** for elasto-plastic materials undergoing infinitesimal deformations is obtained by substituting the strain energy density σ with the work done by internal forces W, [4],[5],[6]

$$\mathbf{G}(l) = -\frac{d}{dl}\int_B W\, da + \int_{\partial B} T\, \nu\cdot\mathbf{u}'\, ds \qquad (5)$$

$G(l)$ is called, in this case, Crack Extension Energy Rate and, if the crack is straight, we have [6]

$$\mathbf{G}(\gamma) = J(\gamma) - \mathbf{e}\cdot\int_L \mathrm{div}(W I - \nabla\mathbf{u}^T T)\, da \qquad (6)$$

In the previous relation, γ is a path around the tip, L is the set enclosed by γ where plastic deformations have taken place and

$$J(\gamma) = \mathbf{e} \cdot \int_{\gamma} (W\mathbf{n} - \nabla\mathbf{u}^T T\,\mathbf{n})\, ds \qquad (7)$$

A closed-form computation of **G** is, in general, not possible; a numerical assessment of **G** starting from a finite element analysis of the cracked body has been carried out[7] and a brief description of it will be given later on in this paper.

The possibility of computing **G** in general load conditions is very useful for applications in the design of structures. Besides, it seems to be possible to collect in the same mathematical framework both the qualification of materials according to fracture mechanics, in which the load applied monotonically increases, and fatigue crack growth in bodies subjected to cyclic loads.

In the application of fracture mechanics to fatigue crack propagation, the crack is considered to be a zero-width saw cut; experiments on real cracks show that a phenomenon of "closure" also exists under cyclic loading with small tensile load; the phenomenon was attributed by Elber[8] to the presence of residual tensile strains along the crack faces during the crack growth process.

The analysis carried out with the present method shows that the closure depends primarily on the effects of residual strains in the ligament of the cracked body, during the phase of decreasing loading. When the load applied increases monotonically, small scale yielding produces a small modification of the Energy Release Rate. In the case of cyclic loading, during the unloading phase, the residual strains formed after a maximum of the load applied is reached give rise to a significant modification of the strain field around the crack tip; consequently, **G** vanishes at a tensile non-zero load.

So the presence of plasticity can never be disregarded, independently of the extension of the plastic region; significant effects on the propagation and retardation of the cracks can also be present in the case of small-scale yielding under cyclic loads.

II. Constitutive relations

In this section we briefly present some results on the infinitesimal theory of plasticity which will be useful later on.[10]

A "deformation process" or, more briefly, a history of duration $\overline{\tau}$ is a continuous and continuously piecewise differentiable mapping, defined on the closed real interval $[0, \overline{\tau}]$ with values in Sym, the space of all symmetric, second-order tensors,

$$\hat{E} : [0, \overline{\tau}] \to \mathrm{Sym}\ , \qquad \tau \mapsto \hat{E}(\tau)\ , \qquad (8)$$

such that

$$\hat{E}(0) = 0\ . \qquad (9)$$

Value $\hat{E}(\tau)$ at instant τ of a history $\hat{E}$ is interpreted as the infinitesimal deformation, that is, the symmetrical part of the displacement gradient, starting from a fixed reference configuration, at a fixed material point. At each instant τ in which $\hat{E}$ is differentiable, $\dot{E}$ represents the value of the derivative of $\hat{E}$ at instant τ.

The materials being considered here are elasto-plastic isotropic solids whose mechanical response to deformation processes is described by a frame-indifferent and rate-independent constitutive functional. For each history $\hat{E}$, $\hat{T}_E(\tau)$ denotes the stress at time τ associated with history $\hat{E}$ by the constitutive functional.

"Elastic range" $\mathbf{E}(\tau)$ at time τ corresponding to history $\hat{E}$ is the closure of an arcwise connected open subset of Sym, whose boundary is attainable from interior points only; it contains $\hat{E}(\tau)$ and its points are interpreted as the infinitesimal deformations from the reference configuration to configurations which are elastically accessible from the current configuration.

Plastic history $\hat{E}^P$ corresponding to $\hat{E}$ is a history such that, for each $\tau \in [0, \overline{\tau}]$, $\hat{E}^P(\tau)$ is a traceless tensor, belongs to $\mathbf{E}(\tau)$ and corresponds to an unstressed configuration.

As usual, it is then supposed there exist two material constants λ and μ such that, if $\hat{E}$ and $\hat{E}^P$ are a history and the corresponding plastic history, respectively, we have, for each $\tau \in [0, \overline{\tau}]$,

$$\hat{T}_E(\tau) = \mathbb{T}[\hat{E}(\tau) - \hat{E}^p(\tau)] = 2\mu(\hat{E}(\tau) - \hat{E}^p(\tau)) + (\lambda \mathrm{tr}\hat{E}(\tau))I \ . \quad (10)$$

For each history $\hat{E}$ and for each $\tau \in [0, \overline{\tau}]$

$$\zeta_E(\tau) = \int_0^\tau \|\dot{E}^p(\tau')\| d\tau' \quad (11)$$

is the length of the path described up to instant τ by the plastic deformation tensor in Sym_0, all traceless element of Sym. ζ is called the Odqvist parameter.

In view of the applications we have in mind, we accept the von Mises criterion, that is to say, we suppose that for each history $\hat{E}$ and for each $\tau \in [0, \overline{\tau}]$ the corresponding elastic range is the cylinder

$$\mathbf{E}(\tau)=\{E \in \mathrm{Sym} \mid \|\hat{E}_0(\tau) - \hat{C}_E(\tau)\| \le \rho(\zeta(\tau))\}, \quad (12)$$

where $\rho : \mathbb{R}^+ \to \mathbb{R}^+$ is a differentiable and non-decreasing material function, $\hat{E}_0(\tau)$ is the traceless part of $\hat{E}(\tau)$ and $\hat{C}_E(\tau)$ is a traceless, symmetric tensor.

Moreover, we suppose that a non-negative constant η exists such that for each history $\hat{E}$ and for each $\tau \in [0, \overline{\tau}]$ we have

$$\hat{C}_E(\tau) = (1 + \eta)\hat{E}^p(\tau) \ . \quad (13)$$

The set of constitutive hypotheses is completed by the flow rule which states that, when $\dot{E}^p(\tau)$ is different from zero, it is parallel to the outward unit normal on the elastic range at $\hat{E}(\tau)_0$.

For each history $\hat{E}$ and for each $\tau \in [0, \overline{\tau}]$, the work done by internal forces in the deformation process $\hat{E}$ up to time τ, is

$$\hat{W}_E(\tau) = \int_0^\tau \hat{T}_E(\tau) \cdot \dot{E}(\tau) d\tau' \ . \quad (14)$$

$\hat{W}_E(\tau)$ can be expressed as an explicit function of $\hat{E}(\tau)$, $\hat{E}^p(\tau)$ and $\zeta(\tau)$[6]:

$$\hat{W}_E(\tau) = 1/2\ (\hat{E}(\tau) - \hat{E}^p(\tau)) \cdot \mathbb{T}[\hat{E}(\tau) - \hat{E}^p(\tau)] + \mu\eta\|\hat{E}^p(\tau)\|^2 + 2\mu\omega(\zeta_E(\tau)) \ , \quad (15)$$

where ω is the primitive of ρ such that $\omega(0) = 0$.

III. Numerical computation of the crack extension energy rate

Let us suppose that body B contains an edge crack, represented at every instant τ by the image of a smooth non-intersecting curve $\hat{\chi}_l : [0,l] \to B$, $\alpha \to \hat{\chi}_l(\alpha)$, parametrized by arc length α. The length $l = l(\tau)$ of curve $\hat{\chi}_l$ is a non-decreasing function of time τ during the motion of B and, therefore, it can be used as a time scale; $\mathbf{e}(\alpha) = d\hat{\chi}_l/d\alpha$ denotes the unit vector field tangent to the crack, and $\mathbf{n}$ is the outward unit normal to γ.

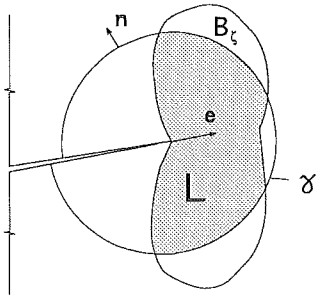

Fig.1 The plastic region B_ζ and the L domain.

Moreover, we assume certain regularity conditions of $\mathbf{u}$, E^p, ζ and W, that body forces are absent and that the crack faces are traction free[2].

For each path γ around the tip, let F be the subset of B enclosed by γ, $B_\zeta = \{x \in B \mid \zeta \neq 0\}$ the plastic region and let $L = F \cap B_\zeta$ as shown in Fig.1, that is the subset of F where plastic deformations have taken place.

If the crack is straight, we have[6]

$$\mathbf{G}(\gamma) = J(\gamma) - \mathbf{e} \cdot \int_L \mathrm{div}(W\mathrm{I} - \nabla\mathbf{u}^T T)da. \quad (16)$$

Assuming $\mathbf{e}$ is parallel to the x_1 axis, because divT = 0, we can write

$$\mathbf{G} = \int_\gamma (W n_1 - t_i u_{i,1})\, ds - \int_L (W_{,1} - \varepsilon_{ij,1}\sigma_{ij})\, da \quad (17)$$

where ε_{ij} and σ_{ij} are the total deformation and stress components.

In order to evaluate $\mathbf{G}$ for elasto-plastic hardening materials, computer code GJINT2D has been implemented at the Department of Aerospace Engineering of the University of Pisa. The code is set up for bidimensional problems.

The computation of **G** with the GJINT2D code can be summarized as follows:

(i) a bidimensional finite element analysis of the body is performed using eight node isoparametric elements; the finite element code used is NO.S.A.[9].

(ii) The integration paths are defined along the Gauss points of the elements, as shown in Fig.2. The integration paths can cross the elements in the various ways shown in fig.3. For any type of crossing, a new element is defined as the portion of the element inside the path and with the Gauss points positioned in accordance with the new boundary.

(iii) The line and surface integrals are computed along the integration paths γ and over the previously defined surface L, respectively. The line and surface integration functions are:

$$F^k_\gamma(\mathbf{x},l) = W n_k - \sigma_{ij} n_j u_{i,k}\,, \qquad k=1,2 \qquad (18)$$
$$F^k_L(\mathbf{x},l) = W_{,k} - (u_{i,k} T_{ij})_{,j}\,,$$

respectively, where:

$$W(\mathbf{x},l) = \sum_{ij}^{2} \mu (\varepsilon_{ij} - \varepsilon^p_{ij})^2 + \frac{\lambda}{2}\left(\sum_{i}^{2}\varepsilon_{ii}\right)^2 + 2\mu\omega(\zeta) + \mu\eta\sum_{ij}^{2}(\varepsilon^p_{ij})^2 \qquad (19)$$

and

$$W_{,i} = \sum_{hj}^{2} 2\mu\,(\varepsilon_{hj} - \varepsilon^p_{hj})\left(\frac{\partial\varepsilon_{hj}}{\partial x_i} - \frac{\partial\varepsilon^p_{hj}}{\partial x_i}\right) + \lambda\left(\sum_{k=1}^{2}\varepsilon_{kk}\right)\left(\sum_{k=1}^{2}\frac{\partial\varepsilon_{kk}}{\partial x_i}\right) + 2\mu\frac{d\omega}{d\zeta}\frac{d\zeta}{dx_i} + \mu\eta\sum_{ij}^{2} 2\varepsilon^p_{ij}\frac{\partial\varepsilon^p_{hj}}{\partial x_i}. \qquad (20)$$

The surface integral is computed in the isoparametric space (ξ,η) ; if f is a function defined on the subset R of the (x,y) plane, we have

$$\int_R f(x,y)dxdy = \int_A \varphi(\xi,\eta)\det(J)d\xi d\eta\,. \qquad (21)$$

where $\varphi(\xi,\eta) = f(x(\xi,\eta), y(\xi,\eta))$, $A = J^{-1}(R)$ and:

$$x = \sum_{i=1}^{8} N_i(\xi,\eta)\, x_i\,, \quad y = \sum_{i=1}^{8} N_i(\xi,\eta)\, y_i,$$

with $N_i(\xi,\eta)$ the shape functions.

The displacement field and its derivatives are obtained by means of the shape functions,

$$\mathbf{u}(\xi,\eta) = \sum_{i=1}^{8} N_i(\xi,\eta)\,\mathbf{u}_i, \qquad (22)$$

$$\frac{\partial\mathbf{u}}{\partial x_j} = \sum_{i=1}^{8}\frac{\partial N_i(\xi,\eta)}{\partial x_j}\mathbf{u}_i = \sum_{i=1}^{8}\left(\frac{\partial N_i(\xi,\eta)}{\partial\xi}\frac{\partial\xi}{\partial x_j} + \frac{\partial N_i(\xi,\eta)}{\partial\eta}\frac{\partial\eta}{\partial x_j}\right)\mathbf{u}_i. \qquad (23)$$

At the Gauss points, the stresses, strains and Odqvist parameter are obtained by finite element analyses; along the lines connecting the Gauss points, the strain components in the (ξ,η) plane are obtained by parabolic interpolations. So the strain derivatives are obtained by means of the derivation rules,

$$\frac{\partial\varepsilon_{ij}}{\partial x} = \frac{\partial f^{(1)}_{ij}}{\partial\xi}\frac{\partial\xi}{\partial x} + \frac{\partial f^{(2)}_{ij}}{\partial\eta}\frac{\partial\eta}{\partial x}, \qquad \frac{\partial\varepsilon_{ij}}{\partial y} = \frac{\partial f^{(1)}_{ij}}{\partial\xi}\frac{\partial\xi}{\partial y} + \frac{\partial f^{(2)}_{ij}}{\partial\eta}\frac{\partial\eta}{\partial y}, \qquad (24)$$

where $f^{(1)}_{ij}(\xi,\eta)$ and $f^{(2)}_{ij}(\xi,\eta)$ are the interpolation functions of strain ε_{ij} along the ξ=cost and η=cost directions, respectively.

The derivatives $\partial\xi/\partial x$ and $\partial\eta/\partial x$ in (24) are elements of the inverse of the jacobian matrix

$$J^{-1} = \begin{bmatrix} \frac{\partial\xi}{\partial x} & \frac{\partial\eta}{\partial x} \\ \frac{\partial\xi}{\partial y} & \frac{\partial\eta}{\partial y} \end{bmatrix}; \qquad (25)$$

the expressions of the components of the J^{-1} matrix are obtained explicitly by means of an appropriate procedure[7].

The computation of the surface integral is rather critical when high gradients of strain are present in the crack-tip region, because of the difficulties in the

interpolation of strains by means of second order polynomians. The numerical analysis performed with the theory of infinitesimal plasticity is valid only when small strains are present at the crack tip.

In the examples shown in this paper, **G** is computed by applying only small values of the external load in order to avoid the presence of large strains at the crack tip. The external load is applied step by step to the cracked body; at any loading step, the Odqvist parameter, the total and plastic strains and the Cauchy stress are computed.

In this paper we assume that the radius ρ of the elastic range is a linear function of ζ,

$$\rho(\zeta) = \frac{\tau_0}{2\mu}\sqrt{2}\,(1 + \beta\,\zeta) \qquad (26)$$

and, then,

$$\omega(\zeta) = \frac{\tau_0}{2\mu}\sqrt{2}\,(\zeta + \beta\,\frac{\zeta^2}{2}). \qquad (27)$$

The constitutive parameters η and β are obtained by uniaxial cyclic tests[10].

IV. Examples.

As a first example, we shall consider a rectangular unstiffened Center Cracked Panel made of steel, 1600 mm long, 800 mm wide and a crack length of 200 mm; the finite element mesh of a quarter of the panel is shown in fig.4, together with the integration paths used for the computation of **G**. The stress-strain curve of the material is approximated by a bilinear function; isotropic hardening is assumed with $\eta=0, \beta=25.0$, $\tau_0=165.8$ MPa, E=214000 MPa (Young modulus). The specimen is loaded with the constant cyclic stress in fig.5, with $R=\sigma_{min}/\sigma_{max}=0$.

Fig.6 shows the **G** values obtained versus the applied stress. The values of the line integral in the loading and unloading phases are nearly the same and, in the case of small scale yielding as in the present example, they are very close to the elastic case. On the other side, even though the values of the surface integral are very small when the load is increasing, they are very significant when load is decreasing (fig.7); the contribution of the surface integral to **G** is negative, in accordance with the fact that the energy absorbed for the formation of the yielded region B_ζ is not available for the extension of the crack.

Fig.6 shows that, owing to the negative contribution of the surface integral, **G** becomes negative during the first unloading phase and, when the load increases in the second cycle, **G** becomes positive only when a certain load, $P_{G=0}$ in fig.6, is exceeded. The same happens in the next cycles due to the contribution of the surface integral.

In the $[0,P_{G=0}]$ loading range, no energy is available for the propagation of the crack, as if the crack were closed; this phenomenon can be defined as "Closure".

According to Elber[8] the closure phenomenon depends on the residual tensile strains in the wake of the plastic region around the crack faces when the crack is growing. According to the present results, a crack closure is obtained independently of the presence of residual strains behind the crack tip (no crack propagation is simulated here); the crucial factor seems to be the formation of the region B_ζ in the ligament, independently of the kinematics of the crack faces.

The second example is a C.C.P. specimen with the same geometry of the first panel, made of 2024-T3 alloy, in the hypothesis of pure kinematic hardening, $\beta=0$, $\eta=0.1$ $\tau_0=187.1$ MPa, E=73000 MPa. The specimen is subjected to the sequence of cyclic loads shown in fig.8, with two groups of five constant amplitude cycles and an intermediate group of three overstress cycles; about 380 increments of load have been applied to carry out the computation of **G**.

Here again we have a crack closure, even though the crack faces are always open. The shape of the crack opening at the end of the overstress cycles, shown in fig.9, appears to be similar to the one observed in experiments.

The **G** values versus the load increments are shown in fig.10. A retardation effect is produced by the presence of the overload cycles, so that the active **G** values in the final group of cycles are significantly lower than those of the first group.

The third examples concern the same

C.C.P. specimen, but with the constitutive constant $\beta=0$, $\eta=0.28$ subjected to loading histories consisting of three groups of three stress cycles, in order to obtain both $R = \sigma_{min} / \sigma_{max} = 0.0$, 0.3 and 0.5, σ_{max} being constant (fig. 11), and $R = 0$ with variable σ_{max} (fig. 12). The computations of **G** are carried out in the cases of pure kinematic hardening and combined hardening.

With the kinematic hardening model and for the loading hystory in fig. 11, a virtually constant decrease of **G** is present at every cycle of the first and second group (R=0.0, R=0.3), as shown in fig.13. In fact, the elastic stress range cannot widen and, then, the energy available for the crack growth decreases at every cycle virtually by the same amount. The decrease of **G** at every cycle equals the increase of the energy absorbed in the B_ζ region. When the range of the applied load becomes sufficiently small, as in the case of R=0.5, the stress remains internal to the elastic stress range and the rate of energy absorbed at every cycle vanishes.

With the same material, but with the load history shown in fig. 12, the **G** values in the second and third block of cycles are negative (fig.14), apart from small positive values in the second block and, therefore, are not available for producing propagation of the crack.

The results shown in fig.15 concern the three blocks of loading at R=0.0, 0.3 and 0.5 (fig.11), and a material with combined hardening ($\beta=25.0$ and $\eta=0.28$). The decrease of **G** for every cycle is lower than the decrease observed for kinematic hardening; after the first three cycles, the second and third blocks are fully active and no further decrease of **G** is present in these two blocks.

All the numerical results presented in this paper show that the computation of the Crack Extension Energy Rate is greatly dependent on the constitutive model.

Acknowledgment:

The present research was supported by the Department of Aerospace Engineering of the University of Pisa, by the CNUCE, Pisa, by the P. Foresio Foundation and by the Italian Ministry of Scientific Research and Technology. The authors gratefully acknowledge the contribution of Marco Oriunno for his help in carrying out the computations.

References

1. Rice J.R."A path independent integral and the approximate analysis of strain concentrations by notches and cracks" J. Appl.Mech., Vol.35, pp 379-386, 1968.
2. Gurtin M."On the energy release rate in quasi-static elastic crack propagation" J. Elasticity, Vol.9, pp 187-195, 1979.
3 Eshelby J. D. "Energy relations and the energy-momentum tensor in continuum mechanics". Inelastic Behavior of Solids, pp 75-115, Ed. by M. F. Kanninen et al., McGraw-Hill, New York 1970.
4 Schmitt W., Kienzler R. "The J-Integral concept for elastic-plastic material behavior". Eng. Fracture Mech., Vol. 32, pp. 409-418, 1989.
5 Moran B., Shih C. H. A general treatment of crack tip contour integrals. Int. J. Fracture, Vol. 35, pp 295-310, 1987.
6 Chiarelli M., Frediani A., Lucchesi M. "On the crack extension Energy rate in elastic plastic Fracture Mechanics". Defect Assessment in Components - Fundamentals and Applications, edited by J.B. Blauel and K.H. Schwalbe - MEP, London, 1991
7 M. Chiarelli, A. Frediani "A computation of the three-dimensional J Integral with a view to applications in fracture mechanics", submitted to Eng. Fracture Mech. for publication
8. Elber W."The significance of fatigue crack closure" ASTM STP 486, pp 230-242, 1971.
9. Degl'Innocenti S., Lucchesi M., Pagni A., Pasquinelli G."Manuale d'uso del programma NOSA", Cnuce, Via S. Maria 26, Pisa, (in italian).
10. Guidotti P., Lucchesi M., Pagni A. "Elastic-plastic behaviour with work-hardening: an appropriate model for structural software" Meccanica, vol. 19, pp43-51, 1984.

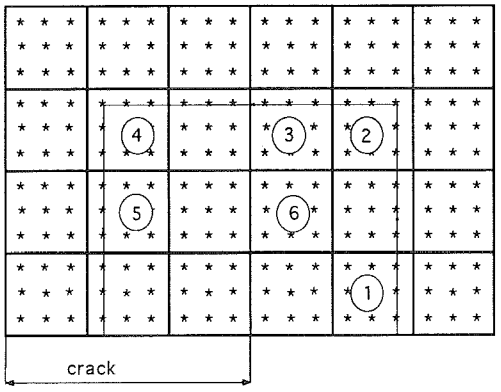

Fig.2 Sketch of a typical integration path.

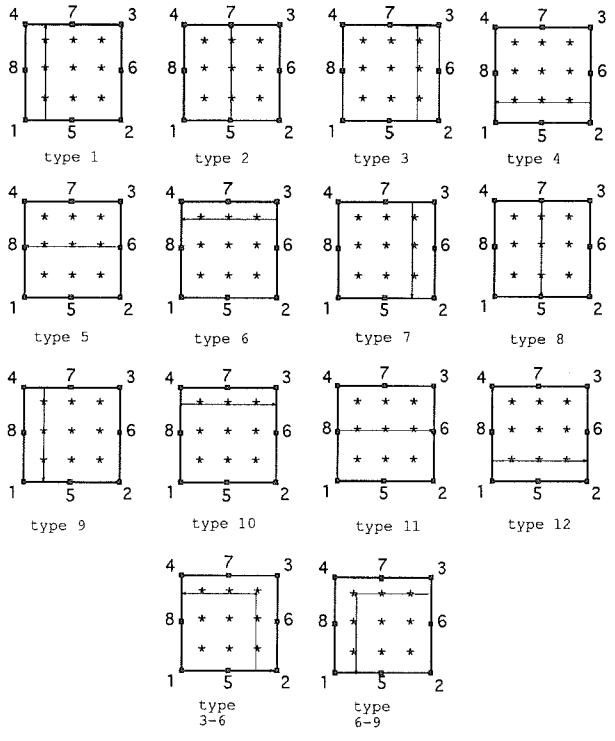

Fig.3 Types of crossing of the integration paths.

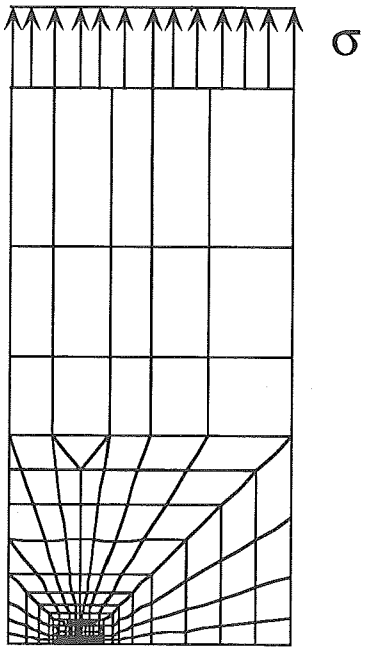

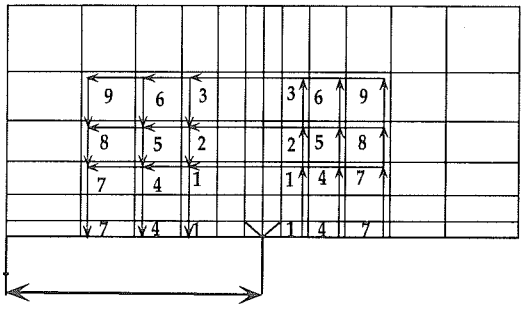

Fig.4 F.E. mesh of a quarter of the panel and positions of the integration paths.

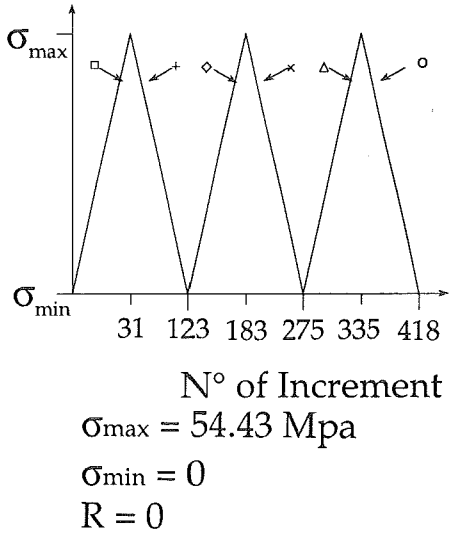

Fig.5 Hystory of the load applied in example 1.

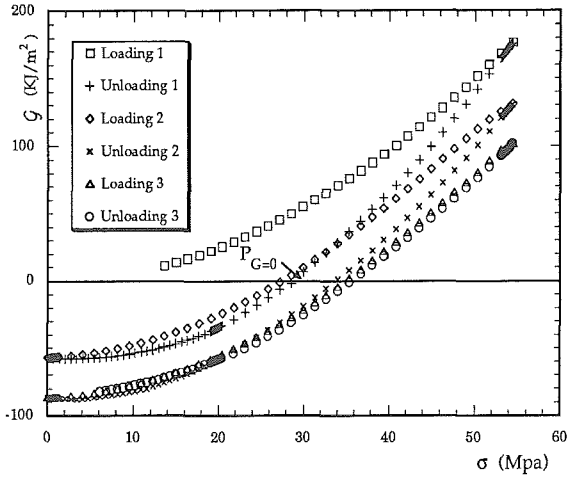

Fig.6 Crack Extension Energy Rate vs load applied for example 1.

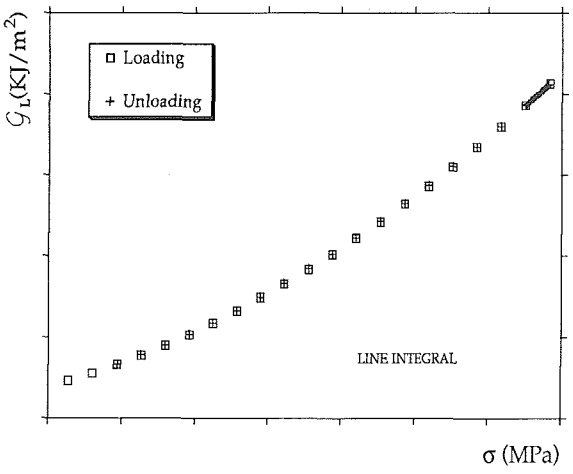

Fig.7a Line integral in example 1.

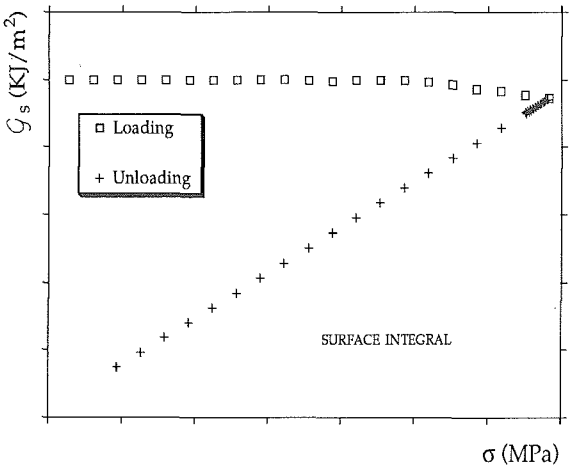

Fig.7b Surface integral in example 1.

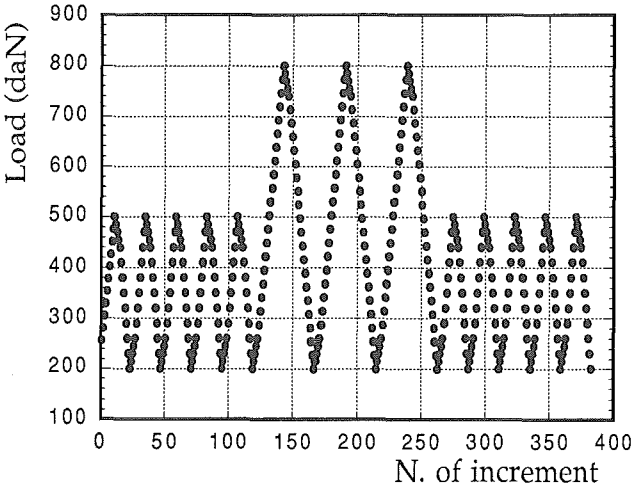

Fig.8 Loading hystory for the specimen made with 2024 Aluminum alloy.

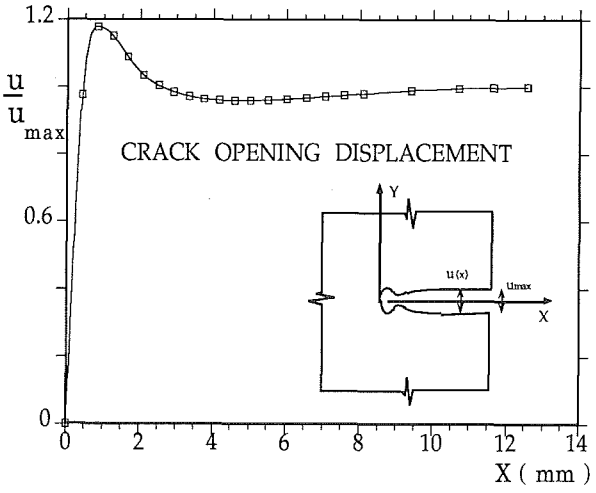

Fig.9 Crack Opening near the crack tip.

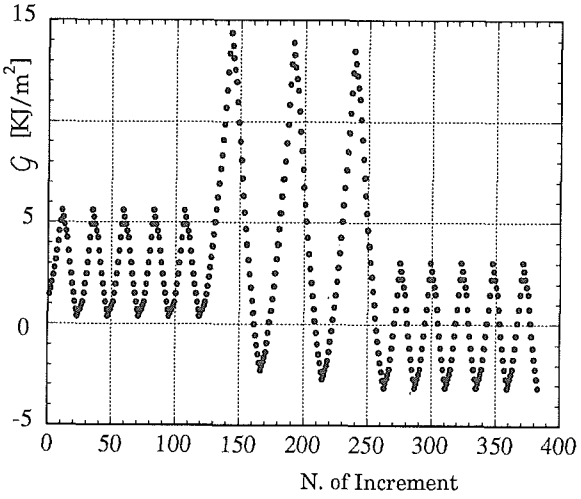

Fig.10 Crack Extension Energy Rate vs load applied in example 2.

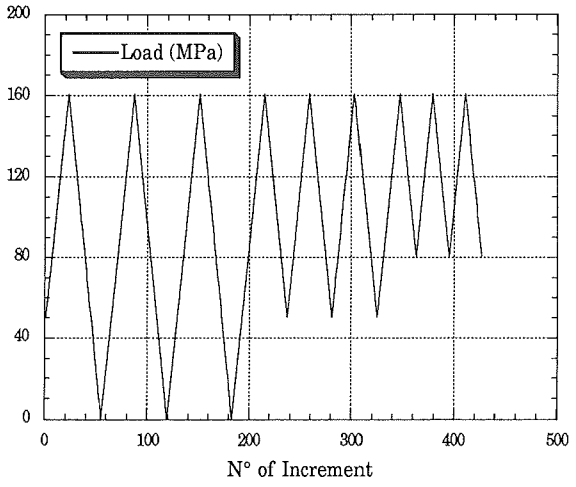

Fig.11 Loading hystory with R = 0.0, 0.3 and 0.5 and variable σ_{min}.

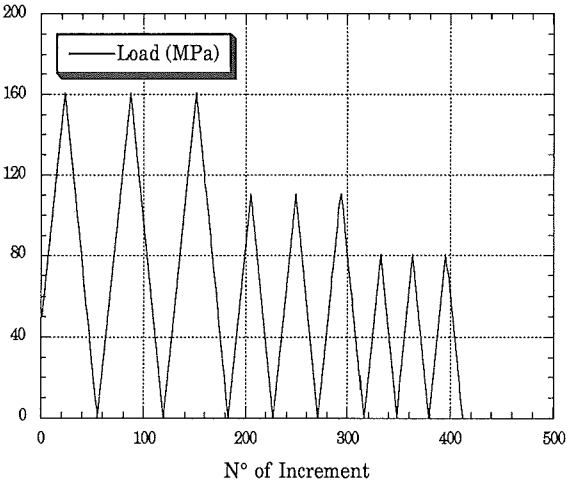

Fig.12 Loading hystory with R = 0.0 and variable σ_{max}

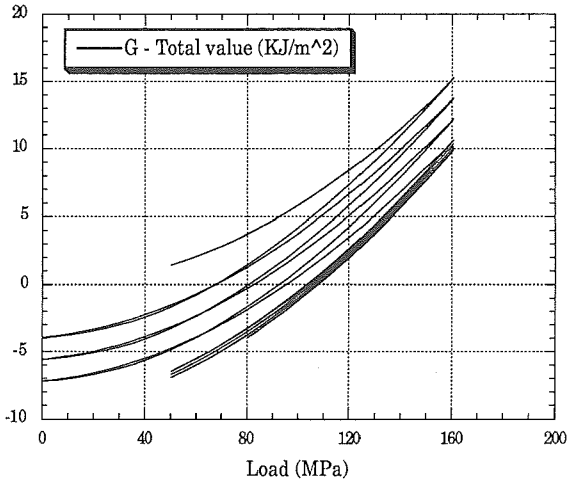

Fig.13 G vs load applied for the loads in fig.11; kinematic hardening.

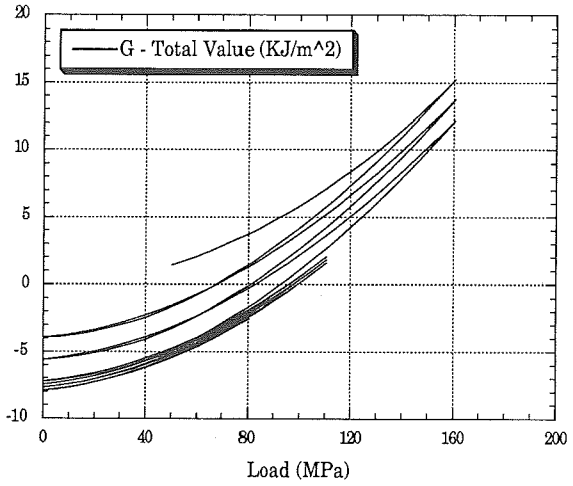

Fig.14 G vs load applied for the loads in fig.12; kinematic hardening.

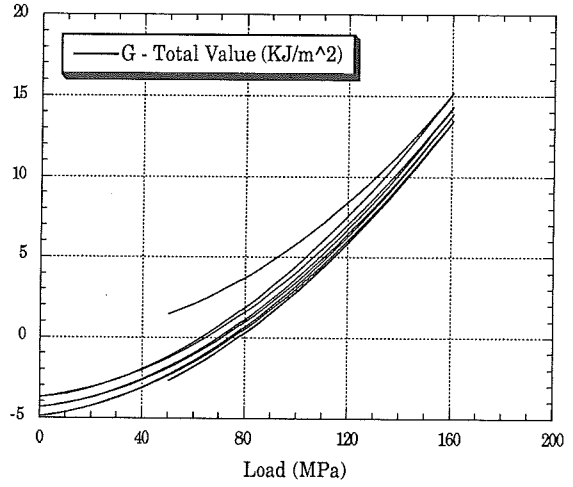

Fig.15 G vs load applied for the loads in fig.11 and combined hardening.